

# Microstructural Characterization of LiNbO<sub>3</sub> and LiNbO<sub>3</sub>:Mn Nanofibers Synthesized by Electrospinning

M.C. Maldonado-Orozco<sup>1</sup>, C. Nava-Dino<sup>1</sup>, J.P Flores-De los Ríos<sup>1</sup>, H. Moreno-Álvarez<sup>1</sup>, M.T. Ochoa-Lara<sup>2</sup> and F. Espinosa-Magaña<sup>2</sup>

<sup>1</sup> Facultad de Ingeniería de la Universidad Autónoma de Chihuahua, Nuevo Campus s/n, Chihuahua, Chih. México 31100

<sup>2</sup> Centro de Investigación de Materiales Avanzados, S.C., Laboratorio Nacional de Nanotecnología. Miguel de Cervantes 120, Complejo Industrial, Chihuahua, Chih., México 31136.

In this work, we synthesized pure and Mn-doped LiNbO<sub>3</sub> nanofibers by the electrospinning method and fully characterized the nanostructures by SEM, DRX, TEM and Raman techniques and compared experimental Raman results with ab initio calculations, to probe lattice site substitution of Mn ions.

For pure LiNbO<sub>3</sub>, the precursor solution consisted of poly(vinylpyrrolidone) (PVP), niobium ethoxide (Nb(OCH<sub>2</sub>CH<sub>3</sub>)<sub>5</sub>) and lithium hydroxide (LiOH), dissolved in acetic acid CH<sub>3</sub>COOH and ethanol C<sub>2</sub>H<sub>5</sub>OH. The ratio of molar composition of lithium hydroxide niobium ethoxide was set to 1:1. On the other hand, for Mn-doped LiNbO<sub>3</sub> nanofibers, the precursor solution consisted of lithium hydroxide LiOH, niobium ethoxide Nb(OCH<sub>2</sub>CH<sub>3</sub>)<sub>5</sub>, manganese acetate Mn(C<sub>2</sub>H<sub>3</sub>O<sub>2</sub>)<sub>2</sub> and poly(vinylpyrrolidone) (PVP), dissolved in acetic acid CH<sub>3</sub>COOH and ethanol C<sub>2</sub>H<sub>5</sub>OH. The ratio of molar composition of lithium hydroxide niobium ethoxide and manganese acetate was set to 1:1:0.025.

In both cases, the solution was heated at 25°C while being stirred during 2 hours and then delivered into a metallic needle at a constant flow rate of 0.3 mL/h by a syringe pump. With an applied high-voltage of 15 kV, producing an electric field of 1x10<sup>5</sup> V/m, the precursor solution jet was accelerated toward the aluminum foil, leading to the formation of LiOH/Nb(OCH<sub>2</sub>CH<sub>3</sub>)<sub>5</sub>/PVP and LiOH/Nb(OCH<sub>2</sub>CH<sub>3</sub>)<sub>5</sub>/Mn(C<sub>2</sub>H<sub>3</sub>O<sub>2</sub>)<sub>2</sub>/PVP fiber composites, for pure and Mn-doped respectively, together with a rapid evaporation of the ethanol.

For the calculation of the phonon modes, the LiNbO<sub>3</sub> structure was represented by a 2x2x2 supercell, with 80 atoms, and the structure was fully relaxed to its equilibrium configurations until the Hellmann-Feynman forces were smaller than 0.001 eV/Å. The Hellmann-Feynman forces were then calculated for displaced atoms, one at a time.

By comparing experimental Raman spectra of pure and Mn-doped LiNbO<sub>3</sub>, and the results of the calculations, we were able to probe Mn ion incorporation into the LiNbO<sub>3</sub> lattice and show that Mn substitutes Li sites.

Figs. 1 shows SEM micrographs of as-spun fibers. Cylindrical and randomly oriented Nb(OCH<sub>2</sub>CH<sub>3</sub>)<sub>5</sub>/LiOH/PVP and LiOH/Nb(OCH<sub>2</sub>CH<sub>3</sub>)<sub>5</sub>/Mn(C<sub>2</sub>H<sub>3</sub>O<sub>2</sub>)<sub>2</sub>/PVP composite fibers were obtained, with diameters in the range 93-163 nm.

Fig. 2 shows XRD patterns from calcined composite fibers, showing the formation of crystalline samples of pure and Mn-doped lithium niobate. However, the presence of Mn in this structure is confirmed by energy-dispersive X-ray spectrometry (EDS), as shown later.

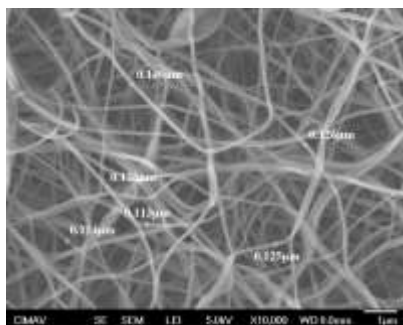
Fig. 3 shows TEM micrographs of necklace-like nanofibers from calcined Mn-doped LiNbO<sub>3</sub>.

Fig. 4a and d shows an EDS mapping through a typical nanofiber, where it can be seen that Mn atoms are uniformly distributed in the structure.

Fig. 5 shows the Raman spectra of the calcined electrospun nanofibers in the spectral range of 100 to 700 cm<sup>-1</sup>, along with calculated LiNbO<sub>3</sub> spectrum.

**References:**

- [1] M.C. Maldonado-Orozco, M.T. Ochoa-Lara, J.E. Sosa-Márquez, S.F. Olive-Méndez, F. Espinosa-Magaña, Synthesis and characterization of electrospun LiNbO<sub>3</sub> nanofibers, *Ceramics International* 41(2015) 14886-14889.
- [2] C.R. Cena, K.B. Ajay, B. Banarji, Structural, dielectric, and electrical properties of lithium niobate microfibers, *Journal of Advanced Ceramics* 5 (2016) 84-92.
- [3] Y. Furukawa, K. Kitamura, A. Alexandrovski, R.K. Route, M.M. Fejer, G. Foulon, Green-induced infrared absorption in MgO doped LiNbO<sub>3</sub>, *Applied Physics Letters* 78 (2001) 1970-1972.



**Fig. 1.** SEM image of as-spun LiOH/Nb(OCH<sub>2</sub>CH<sub>3</sub>)<sub>5</sub>/PVP fiber composite.

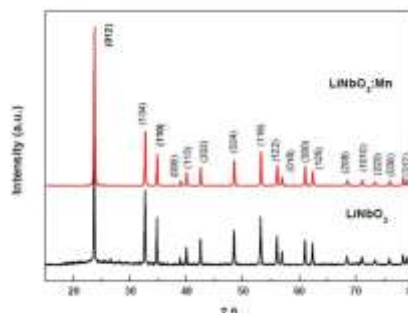


**Fig. 2.** XRD patterns of calcined pure and doped LiNbO<sub>3</sub>.

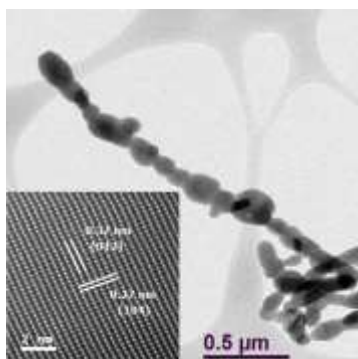


**Fig. 3.** TEM image of Mn-doped LiNbO<sub>3</sub> nanofibers.

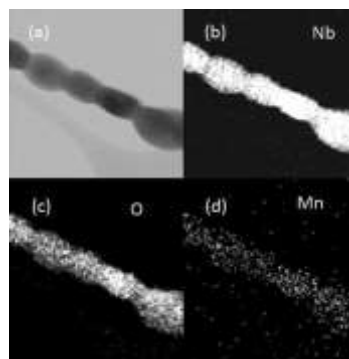


**Fig. 4a-4d.** EDS mapping through a typical nanofiber.

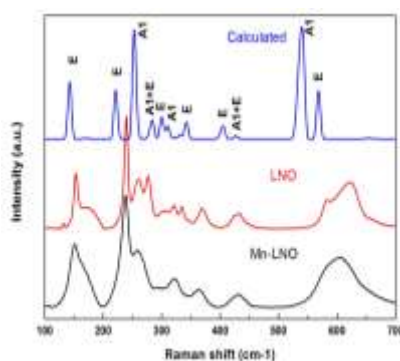


**Fig. 5.** Raman spectra of calculated, pure and Mn-doped LiNbO<sub>3</sub> nanofibers.



(/MandM/2017/)



## Post-Deadline Posters

The post-deadline poster submission deadline has passed. No additional submissions are being accepted at this time. We look forward to seeing your work at M&M 2018 in Baltimore.

Click on each paper title to link to the original 2-page paper. All Post-Deadline Papers below will be presented as Posters on Monday, August 7, 2017 from 3-5 PM, in the poster area of the M&M 2017 Exhibit Hall.

Post-deadline papers are not included in the program or proceedings.

Board Number	Presenter Name	Paper Title
PDP-1	Siddardha Koneti	Rapid Tomography in Environmental TEM: Solutions for a Fast Analysis of Nano-Materials in 3D Under in situ Conditions (abstracts/PDP-01_Koneti.pdf)
PDP-2	Siddardha Koneti	Real time 3D Environmental TEM In-depth Study of Catalytic Soot Combustion on Zirconia-based Catalysts (abstracts/PDP-02_Koneti.pdf)
PDP-3	Justin Ondry	Dynamics and Removal Pathway of $b=1/2 \langle 110 \rangle$ Edge Dislocations in Imperfectly Attached PbTe Nanocrystals; Towards Design Rules for Oriented Attachment (abstracts/PDP-03_Ondry.pdf)
PDP-4	Jacques Gierak	FIB Nanowriter Developments: Challenging the Paradigm, Progress, and Perspectives (abstracts/PDP-04_Gierak.pdf)
PDP-5	Zhiya Dang	Temperature Dependent Study of Electron Beam-induced Transformation of Cesium Lead Halide Perovskite Nanocrystals (abstracts/PDP-05_Dang.pdf)
PDP-6	Thomas Albrecht	Chemical Mapping at the Nanoscale by Photo-induced Force Microscopy (abstracts/PDP-06_Albrecht.pdf)
PDP-7	Eiji Usukura	A Cryosectioning Technique for the Observation of Intracellular Structures and Immunocytochemistry of Tissues in Atomic Force Microscopy (AFM) (abstracts/PDP-07_Usukura.pdf)
PDP-8	K. N. Tran	Microstructural Evolution of Reverse Sensitization Heat Treatment of Aluminum 5456 (abstracts/PDP-08_Tran.pdf)
PDP-9	Nasser Hamden	Microanalysis of Fine and Ultrafine Indoor Aerosol Pollutants in Sharjah, UAE (abstracts/PDP-09_Hamdan.pdf)
PDP-10	Priyanka Anand	Low Temperature Electron Diffraction Studies of the Verwey Transition of Magnetite (abstracts/PDP-10_Anand.pdf)
PDP-11	Ji Hee Kwon	Observation of Hematite with Various Shapes by Scanning Electron Microscopy (abstracts/PDP-11_Kwon.pdf)

[Registration Information \(/MandM/2017/registrati](/MandM/2017/registrati)

[Full Scientific Program \(/MandM/2017/program/Sci](/MandM/2017/program/Sci)



(<http://www.microscopy.org/>)



(<http://www.microanalysisociety.org/>)



(<http://www.fieldemission.org/>)

PDP-12	Dennis Paul	Auger Electron Spectroscopy Analysis of Fresh and Aged Alumina Supported Silver Catalysts (abstracts/PDP-12_Newman.pdf)
PDP-13	Eric Formo	Utilizing STEM for the Determination of How Morphology Affects the Aging Mechanism of Ag Nanostructures in Aquatic Environments (abstracts/PDP-13_Formo.pdf)
PDP-14	Zhi-Peng Li	Quantitative FIB-SEM 3D Tomography for Failure Analysis in Data Storage Industry (abstracts/PDP-14_Li.pdf)
PDP-15	Andreas Geiger	Sparse Sampling Image Reconstruction In Lissajous Beam-scanning Microscopy (abstracts/PDP-15_Geiger.pdf)
PDP-16	Shogo Kataoka	Wide Area Cross-section Milling by Using Cross Section Polisher (abstracts/PDP-16_Kataoka.pdf)
PDP-17	Caleb Carreño-Gallardo	Effect of Multiwall Carbon Nanotubes (MWCNs) Reinforcement on the Mechanical Behavior of Synthesis 7075 Aluminum Alloy Composites by Mechanical Milling (abstracts/PDP-17_Carreno-Gallardo.pdf)
PDP-18	Mei-li Qi	In situ TEM Visualization of Superior Nanomechanical Flexibility of an Individual Hydroxyapatite Nanobelt (abstracts/PDP-18_Qi.pdf)
PDP-19	Yuki Sasaki In-situ	Observation of Individual Ferritin Molecules in Graphene Sandwiched Structure (abstracts/PDP-19_Sasaki.pdf)
PDP-20	Ryuji Yoshida	Simulation investigation of Compact Cs/Cc Corrector with Annular and Circular Electrodes for SEM (abstracts/PDP-20_Yoshida.pdf)
PDP-21	Francisco Capani	Alteration in Synapses Induced by Perinatal Asphyxia (abstracts/PDP-21_Capani.pdf)
PDP-22	 M.C. Maldonado-Orozco	Microstructural Characterization of LiNbO <sub>3</sub> and LiNbO <sub>3</sub> :Mn Nanofibers Synthesized by Electrospinning (abstracts/PDP-22_Maldonado.pdf)
PDP-23	Rayne Lim	Ultrastructural Retinal Neuronal Changes in Juvenile Miniature Ossabaw Pigs Fed a Western Diet (abstracts/PDP-23_Lim.pdf)
PDP-24	Josef Brown	Water Vapor Assisted Electron Beam Patterning of PMMA (abstracts/PDP-24_Brown.pdf)
PDP-25	James Torres	Characterization of Hydrophilic Cupric Oxide Nanostructures - Towards Tunable Vitreous-Ice Film Thickness (abstracts/PDP-25_Torres.pdf)
PDP-26	Kun-Lin Lin	Interfacial Characterization of Metals/GaSb Contacts using Transmission Electron Microscopy (abstracts/PDP-26_Lin.pdf)
PDP-27	Jiangtao Zhu	Electron Vortex Beam Characterization of L10 FePt Nanograins (abstracts/PDP-27_Zhu.pdf)
PDP-28	Ismail Oztel	Segmentation of Mitochondria in Electron Microscopy Volumes using Deep Learning (abstracts/PDP-28_Oztel.pdf)
PDP-29	Mark Homer	Preparation of Bismuth Telluride Specimens for TEM (abstracts/PDP-29_Homer.pdf)
PDP-30	Jan Ruzs	Delocalization of Magnetic Scattering Intensity in Spectrum Images Measured with Atomic Size Electron Beams (abstracts/PDP-30_Ruzs.pdf)

PDP-31	Haw-Tyng Huang	Phase Identification of Acetylene Benzene Cocystal Derived Carbon Nanophases (abstracts/PDP-31_Huang.pdf)
PDP-32	Anna Pittman	Enhancing the Precision of Biophysical Force Spectroscopy Assays using Focused Ion Beam Modified Cantilevers (abstracts/PDP-32_Pittman.pdf)
PDP-33	M.C. Maldonado-Orozco	Nanofibers Synthesized by Electrospinning: Microstructural Characterization of BaTiO <sub>3</sub> and Mn doped (abstracts/PDP-33_Maldonado.pdf)
PDP-34	Karl Hujsak	High Speed Analytical Electron Microscopy with Machine Learning and Dynamic Sampling (abstracts/PDP-34_Hujsak.pdf)
PDP-35	Gianpiero Torraca	Progress Towards 21 CFR Part 11 Data Integrity Compliance in a GMP Environment of a Forensics Lab in the Pharmaceutical/Biopharmaceutical Industry (abstracts/PDP-35_Torraca.pdf)
PDP-36	Gi-Yeop Kim	STEM-EELS Observation of Particular Ferroelectric State in the PbTiO <sub>3</sub> /SrTiO <sub>3</sub> Superlattice film (abstracts/PDP-36_KimG.pdf)
PDP-37	Yuanyuan Zhu	Application of STEM Diffraction Contrast Imaging and Chemical Analysis for a Comprehensive Characterization of Nuclear Reactor Structural Alloys (abstracts/PDP-37_Zhu.pdf)
PDP-38	Anette von der Handt	Improving EPMA Analysis of Beam-Sensitive Materials by a Combined Mapping and Time-Dependent Intensity Correction Approach (abstracts/PDP-38_vdHandt.pdf)
PDP-39	Zhengyang Wang	Transmission Electron Microscopy Microanalysis of Various Iron-based Carbonaceous Sorbents for Arsenate Adsorption (abstracts/PDP-39_Wang.pdf)
PDP-40	Mariia Goriacheva	Chemically Induced Controlled Growth of CsPbBr <sub>3</sub> Perovskite Nanocrystals (abstracts/PDP-40_Goriacheva.pdf)
PDP-41	Jian-Guo Zheng	A Combination of Focus Ion Beam and NanoMill for TEM Specimen Preparation (abstracts/PDP-41_Zheng.pdf)
PDP-42	Alice Greenberg	Manipulation of Nanoparticles in Liquid Cell Transmission Electron Microscopy via Electron Vortex Beams (abstracts/PDP-42_Greenberg.pdf)
PDP-43	Patrick Price	Converting the in situ Ion Irradiation TEM into a Dynamic TEM (abstracts/PDP-43_Price.pdf)
PDP-44	M.J. Lagos	Electron Energy-Gain Processes in Nanostructures induced by Fast Electrons (abstracts/PDP-44_Lagos.pdf)
PDP-45	Brian Shevitski	Mapping Crystallographic Order in Pseudo-2D Chalcogenide Thin Films (abstracts/PDP-45_Shevitski.pdf)
PDP-46	Jason Holm	Angularly-Selective Diffraction Imaging Using an Individually Addressable Micromirror Array (abstracts/PDP-46_Holm.pdf)
PDP-47	A.R. Mazza	Investigating Hydrogenation at the Interface of SiC(000-1) and Graphene via Cross Sectional High Resolution Transmission Electron Microscopy (abstracts/PDP-47_Mazza.pdf)
PDP-48	Alec Day	Advanced Reconstruction and Crystallographic Analysis in Atom Probe Tomography (abstracts/PDP-48_Day.pdf)

PDP-49	Narahari Akkaladevi	Flexible Hinges in Bacterial Chemoreceptors (abstracts/PDP-49_Akkaladevi.pdf)
PDP-50	Andrew Muenks	Preliminary EM Studies of Bacterial Phosphoglucosamine Mutase (abstracts/PDP-50_Muenks.pdf)
PDP-51	Hyosun Choi	The Lysosomal Positioning of mTOR Regulator and Regulation of Autophagy (abstracts/PDP-51_Choi.pdf)
PDP-52	Steven Goodman	Fast, Walk-away, Automated Processing of Mammalian Tissue for LM and TEM (abstracts/PDP-52_Goodman.pdf)
PDP-53	Xavier Heiligstein	The HPM Live $\mu$ - From Live Cell Imaging to High Pressure Freezing in Less than 2 Seconds for Correlative Microscopy Approaches (abstracts/PDP-53_Heiligenstein.pdf)
PDP-54	Jia Hao Yeo	Can You Pass Some Mitochondria? Do Erythroblasts Share Mitochondria During Red Blood Cell Production? (abstracts/PDP-54_Yeo.pdf)
PDP-55	Karen Kirby	Discovery and Characterization of Antivirals Targeting the Hepatitis B Virus Capsid with a Novel Mechanism Action (abstracts/PDP-55_Kirby.pdf)
PDP-56	Steven Goodman	Preparing LR White Embedded Tissue with mPrep/s Specimen Capsules (abstracts/PDP-56_Goodman.pdf)
PDP-57	Megan Haney	Establishing TEM Markers of Laryngeal Nerve Injury in a Translational Mouse Model (abstracts/PDP-57_Haney.pdf)
PDP-58	Erica Majumder	Visualization of Adsorption, Absorption and Precipitation of Uranium Minerals by Environmental Bacteria for Bioremediation of Radionuclide-Contaminated Sites (abstracts/PDP-58_Majumder.pdf)
PDP-59	Melainia McClain	Rapid Automated en Bloc Staining for SEM of Sections (abstracts/PDP-59_McClain.pdf)
PDP-60	Babak Shalchi Amirkhiz	Structure-properties Relationship of Ultrafine-grained V-microalloyed Dual Phase Steels (abstracts/PDP-60_Amirkhiz.pdf)
PDP-61	Berit Goodge	Atomic Resolution Rapid Spectroscopic Mapping By Direct Electron Detection (abstracts/PDP-61_Goodge.pdf)
PDP-62	Hanseung Lee	Cryogenic Electron Microscopy (Cryo-EM) Studies: Structure and Formation of Self-assembled Nanostructures in Solution (abstracts/PDP-62_Lee.pdf)
PDP-63	Ashish Suri	A Miniature Electron Energy Analyzer for the Scanning Electron Microscopes (abstracts/PDP-63_Suri.pdf)
PDP-64	Anna Ceguerra	Atom Probe Study of a Stable Al-Mn-Pd Quasicrystal (abstracts/PDP-64_Ceguerra.pdf)
PDP-65	Toby Sanders	Alignment and Autofocusing Techniques for Electron Tomography (abstracts/PDP-65_Sanders.pdf)
PDP-66	Xiaoqiang Qi	Autophagy Contributing to Tumor Recurrence after Radiofrequency Ablation in a Clinically Relevant Murine Model of HCC (abstracts/PDP-66_Qi.pdf)
PDP-67	Abigail Lindstrom	An Easy Preparation is Not Necessarily the Best Preparation (abstracts/PDP-67_Lindstrom.pdf)

PDP-68	Kyun Seong Dae	Direct Observation of Calcium Carbonate Precipitation Using in situ Liquid Transmission Electron Microscopy (abstracts/PDP-68_Dae.pdf)
PDP-69	Kenneth Fahy	Development of a Commercial Laboratory Scale Soft X-ray Microscope (abstracts/PDP-69_Fahy.pdf)
PDP-70	Benjamin Bammes	New Improvements in Direct Detection for TEM (abstracts/PDP-70_Bammes.pdf)
PDP-71	Tim Prost	Persistence of Inhomogeneity from Feedstock Powder to Resulting Electron Beam Additive Manufactured Builds in Ni-based Superalloys (abstracts/PDP-71_Prost.pdf)
PDP-72	Arthur McCray	Oriental Disorder in Epitaxially Connected Quantum Dot Solids (abstracts/PDP-72_McCray.pdf)
PDP-73	Brandi Lee MacDonald	SEM Methods for Pigment Characterization of Pictograph Fragments (abstracts/PDP-73_MacDonald.pdf)
PDP-74	Said Mansour	Correlative and in-situ Materials Imaging and Characterization Capabilities at HBK University in Qatar (abstracts/PDP-74_Said.pdf)
PDP-75	Nabraj Bhattarai	Beam-driven Chemistry in Suspensions of PbTe Nanocrystals using in situ Liquid Cell TEM (abstracts/PDP-75_Bhattarai.pdf)
PDP-76	Kiminori Toyooka	Effective Detection of Fluorescence-labeled Plant Organelles in Resin Section using MirrorCLEM with FE-SEM (abstracts/PDP-76_Toyooka.pdf)
PDP-77	Asher Kantor	Arbovirus Dissemination Across the Midgut Basal Lamina, a Barrier To Arbovirus Infection of <i>Aedes aegypti</i> (abstracts/PDP-77_Kantor.pdf)
PDP-78	Rui Zhang	Probing Morphology and Cellular Processing of Peptide Amphiphile Micelle Vaccines Utilizing Electron Microscopy (abstracts/PDP-78_Zhang.pdf)
PDP-79	Timothy Pegg	Remodeling of Pectic Polysaccharides in <i>Pisum sativum</i> Root Cortical Cells during Hypoxia-induced Aerenchyma Formation (abstracts/PDP-79_Pegg.pdf)
PDP-80	Murugesan Raju	Effect of Smoke Extracts on the Structure and Function of Mitochondria (abstracts/PDP-80_Raju.pdf)

## 2017 Sponsors



Copyright © 2017 Microscopy Society of America

11130 Sunrise Valley Drive, Suite 350, Reston, VA 20191 – Tel: (703) 234-4115

Fax: (703) 435-4390 Email: Association Management (<mailto:AssociationManagement@microscopy.org>)

[Terms of Use \(/terms.cfm\)](#)